Study of Inelastic Scattering of Protons from Sn^{116}, Sn^{122}, and Sn^{124} at Isobaric Analog Resonances*

E. J. SCHNEID,† E. W. HAMBURGER,‡ AND B. L. COHEN
University of Pittsburgh, Pittsburgh, Pennsylvania
(Received 4 May 1967)

Inelastic scattering of protons from targets of Sn^{116}, Sn^{122}, and Sn^{124} was studied with solid-state detectors at the resonances which are isobaric analog states of the $s_{1/2}$ and $d_{3/2}$ single-quasiparticle states of Sn^{117}, Sn^{123}, and Sn^{125}, respectively. Angular distributions were measured on and off the resonances. Sums of inelastic partial widths $\sum\Gamma_{p'}$ are extracted from the data and compared with theoretical predictions from the shell-model calculations of Baranger, Baranger, and Kuo; the over-all agreement is quite good. In particular, the strong transitions observed to excited states at approximately 2.5-MeV excitation in the target nucleus are predicted by the theory. The transition to the collective 3^- state does not show resonances.

I. INTRODUCTION

THE observation of the formation and decay of isobaric analog resonances constitutes an important new tool for nuclear-structure studies in nuclei. By bombarding, for example, Sn^{116} with protons, resonances in the compound nucleus Sb^{117} which are isobaric analog states of the levels of Sn^{117} are formed. The decay of the compound states to various excited levels of Sn^{116} yields information on the parentage of the Sn^{117} states to the excited Sn^{116} levels. More specifically, one can extract the spectroscopic factors for the decay of the Sb^{117} compound states to the states of Sn^{116} by proton emission. If the Sb^{117} resonances were perfect isobaric analog states of the "parent" states in Sn^{117}, then these spectroscopic factors should be proportional to the spectroscopic factors for removing a neutron from Sn^{117} while it is in the "parent" state, leaving Sn^{116} in the same excited states. These spectroscopic factors cannot be measured directly in other reactions.

The purpose of the present experiment was to extract this type of information for the tin isotopes and check whether the results are consistent with other information concerning these nuclei. The tin isotopes were chosen as targets because they have been extensively studied by means of deuteron stripping and pickup experiments at this laboratory,[1,2] and because elaborate shell-model calculations on these nuclei have been performed,[3] yielding wave functions from which spectroscopic factors can be calculated for comparison with experiment.

The isobaric analog resonances observed in the elastic scattering of protons from all the tin isotopes have been studied by Richard, Moore, Becker, and Fox.[4] Allan and co-workers[5–7] studied the inelastic scattering for targets for Sn^{118} and Sn^{120}. In the present experiment, we measure inelastic scattering from Sn^{116}, Sn^{122}, and Sn^{124}. Two resonances are studied in each isotope, corresponding to the low-lying $\frac{1}{2}^+$ and $\frac{3}{2}^+$ states in Sn^{117}, Sn^{123}, and Sn^{125}. The $\frac{1}{2}^+$ is, to a good approximation, a single-quasiparticle $s_{1/2}$ state while the $\frac{3}{2}^+$ is a single-quasiparticle $d_{3/2}$ state.

II. EXPERIMENTAL PROCEDURE

The experiment was carried out with a proton beam from the University of Pittsburgh tandem Van de Graaff. The beam energy was determined by a 90° magnet; the calibration, based on the $C^{13}(p,n)$ threshold energy, is probably accurate within ±10 keV. Two NaI scintillation counters were mounted at the periphery of the chamber at ±25° to the beam in order to monitor the elastically scattered protons from the target during the course of a run. The beam current was collected in a Faraday cup connected to an integrator.

The self-supporting targets of Sn^{116}, Sn^{122}, and Sn^{124} were obtained commercially.[8] The thicknesses of the targets used ranged from 250 to 500 $\mu g/cm^2$; the isotopic enrichments were greater than 90%.

The scattered protons from the target were detected by two 1-mm silicon surface-barrier detectors mounted on a remotely controlled, motorized turntable which could be rotated during the course of the experiment. The pulses from the detectors were fed to linear amplifiers. The pulses from each amplifier were pulse-height analyzed by Nuclear Data 4096 multichannel analyzers. Only 256 channels were used to display a single spectrum. The resolution obtained during the course of the experiment was approximately 40 keV. Permanent magnets set in front of the detectors improved the resolution by preventing low-energy electrons from the target from reaching the detectors. The

* Supported by the National Science Foundation.
† Present address: Physics Department, Rutgers, The State University, New Brunswick, New Jersey.
‡ On leave from Universidade de São Paulo, Faculdade de Filosofia, P. O. Box 8105, São Paulo, Brazil.
[1] B. L. Cohen and R. E. Price, Phys. Rev. **121**, 1441 (1961).
[2] E. J. Schneid, A. Prakash, and B. L. Cohen, Phys. Rev. **156**, 1316 (1967).
[3] T. T. S. Kuo, E. Baranger, and M. Baranger, Nucl. Phys. **79**, 513 (1966).
[4] P. Richard, C. F. Moore, J. A. Becker, and J. D. Fox, Phys. Rev. **145**, 971 (1966).
[5] D. L. Allan, Phys. Letters **14**, 311 (1965).
[6] D. L. Allan, G. A. Jones, G. C. Morrison, R. B. Taylor, and R. B. Weinberg, Phys. Letters **17**, 56 (1965).
[7] D. L. Allan, G. A. Jones, R. B. Taylor, and R. B. Weinberg, Phys. Letters **21**, 197 (1966).
[8] Targets were obtained from Fodor Accelerator Targets, Inc., Pittsburgh, Pennsylvania.

continuous background in the inelastic proton spectra was reduced considerably by preventing the incident beam from hitting any slits near the scattering chamber. The illuminated area of the target was defined by two round apertures, 6.4 mm in diameter and approximately 36 and 60 cm in front of the target, respectively. When more than 1% of the beam hit the apertures the run was stopped.

On the other hand, background was reduced by employing large-area detectors. The defining apertures in front of the detectors were $D=12.7$ mm in diameter. The ratio of the number of particles which enter the detector after being scattered at the edges of the defining aperture to the total number of particles counted is of course proportional to $1/D$.

Excitation functions of the inelastic proton groups were measured at the laboratory angles of 135° and 165°. At the resonance energies corresponding to the $\frac{1}{2}^+$ and $\frac{3}{2}^+$ isobaric analog states, angular distributions were measured from 50° to 165°. Angular distributions over the same angular region were also measured at energies below, in between, and above these two isobaric analog resonance energies.

The cross sections for the inelastic proton groups were measured relative to the monitor detectors, and it was assumed that the cross section for the elastically scattered protons in the monitors was given by the Rutherford formula. This assumption should be valid at the energies (7–8 MeV) used in this experiment. The absolute cross sections measured at the resonance energies are believed to be correct within ±20%.

TABLE I. The experimental results for the $Sn^{116}(p,p')$ reaction. This table lists the excitation energies of the excited states of the target nucleus reached by proton decay from the isobaric analog states, the assigned J^π, and, for each resonance, the absolute cross sections measured at 135° and the sums of the inelastic proton partial widths. Column 1 lists the excitation energies for the levels observed by Allan *et al.* (Ref. 9) with the (p,p') reaction at 11 MeV.

			$Sn^{116}(p,p')$ $\frac{3}{2}^+$, $E_p^{c.m.}=7.02$ MeV		$\frac{1}{2}^+$, $E_p^{c.m.}=6.87$ MeV	
Allan[a] E^* (MeV)	E^* (MeV)	J^π	$d\sigma/d\Omega$ (μb/sr)	$\sum_{lj}\Gamma_{p'lj}$ (keV)	$d\sigma/d\Omega$ (μb/sr)	$\sum_{lj}\Gamma_{p'lj}$ (keV)
1.291	1.29	2^+	734	1.65	325	0.63
1.702	1.76	0^+	62	0.17	159	0.56
	2.03	0^+	22	0.06	120	0.42
2.108						
2.224	2.24		403	1.10	77	0.27
2.267	2.27	3^-				
	(2.31)					
2.366						
2.391						
2.531						
	2.60		274	0.75	100	0.35
2.649						
2.803						
2.845	2.87		91	0.25		

[a] Reference 9.

TABLE II. The experimental results for the $Sn^{122}(p,p')$ reaction. See also caption for Table I.

			$Sn^{122}(p,p')$ $\frac{3}{2}^+$, $E_p^{c.m.}=7.68$ MeV		$\frac{1}{2}^+$, $E_p^{c.m.}=7.82$ MeV	
Allan[a] E^* (MeV)	E^* (MeV)	J^π	$d\sigma/d\Omega$ (μb/sr)	$\sum_{lj}\Gamma_{p'lj}$ (keV)	$d\sigma/d\Omega$ (μb/sr)	$\sum_{lj}\Gamma_{p'lj}$ (keV)
1.142	1.14	2^+	600	2.75	144	0.80
2.103	2.08	(0^+)			67	0.53
2.115						
2.239						
2.260						
2.336						
2.418	2.41		360	2.06	120	0.95
2.496	2.50	3^-				
	2.68	(0^+)			265	2.1
	2.75		86	0.46		
2.870	2.86		205	1.15	57	0.45
3.128	3.14					

[a] Reference 9.

III. EXPERIMENTAL RESULTS

The $\frac{1}{2}^+$ and $\frac{3}{2}^+$ isobaric analog resonances in Sb^{117}, Sb^{123}, and Sb^{125} corresponding to the $s_{1/2}$ and $d_{3/2}$ neutron single-quasiparticle states in Sn^{117}, Sn^{123}, and Sn^{125} were studied using the (p,p') reaction. Tables I, II, and III list the experimental results at the $\frac{1}{2}^+$ and $\frac{3}{2}^+$ isobaric analog resonances for the targets Sn^{116}, Sn^{122}, and Sn^{124}, respectively. These tables list the excitation energies of the excited states of the target nucleus reached by inelastic proton decay from the isobaric analog states, the assigned J^π, and, for each resonance, the absolute differential cross sections measured at 135° and the sums of the inelastic proton partial widths, $\sum_{lj}\Gamma_{p'lj}$, obtained from a Breit-Wigner analysis of the data. The method used to determine $\sum_{lj}\Gamma_{p'lj}$ will be discussed below. For comparison, the first column in each table lists the excitation energies for the levels observed by

TABLE III. The experimental results for the $Sn^{124}(p,p')$ reactions. See also caption for Table I.

			$Sn^{124}(p,p')$ $\frac{3}{2}^+$, $E_p^{c.m.}=7.84$ MeV		$\frac{1}{2}^+$, $E_p^{c.m.}=8.04$ MeV	
Allan[a] E^* (MeV)	E^* (MeV)	J^π	$d\sigma/d\Omega$ (μb/sr)	$\sum_{lj}\Gamma_{p'lj}$ (keV)	$d\sigma/d\Omega$ (μb/sr)	$\sum_{lj}\Gamma_{p'lj}$ (keV)
1.132	1.13	2^+	500	3.2	139	0.70
2.105	2.12		46	0.33		
2.133						
2.199	2.20		70	0.50		
2.217						
2.43	2.43		372	2.70	110	0.65
2.605	2.59	3^-				
2.678	2.69	(0^+)	138	1.0	465	2.8
2.708						
2.879	2.85		248	1.8	107	0.65
2.952						
2.988						
3.215	3.19					

[a] Reference 9.

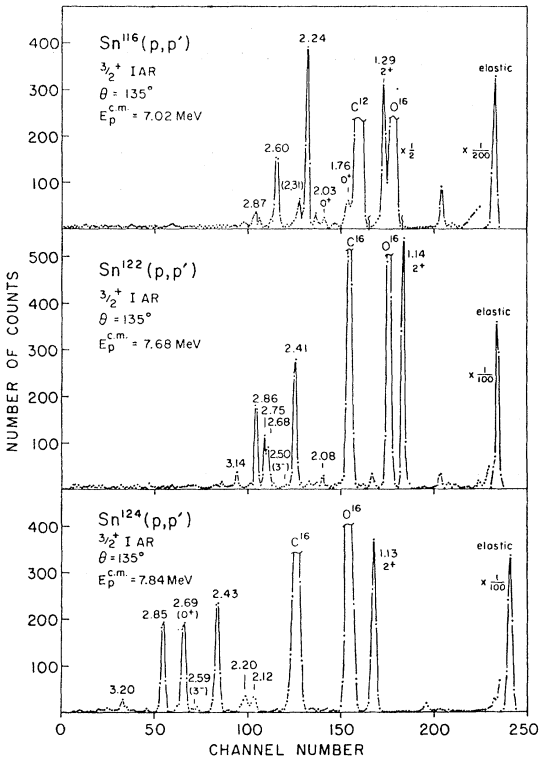

FIG. 1. The proton spectra at 135° measured at the $\frac{3}{2}^+$ isobaric analog resonance energies.

Allan, Armitage, and Doran,[9] who studied the (p,p') reaction at 11 MeV.

Excitation functions of the inelastic proton groups were measured at the laboratory angles 135° and 165°, with 20-keV energy steps over the energy region corresponding to the two resonances. Figure 1 shows the proton spectra at 135° measured at the $\frac{3}{2}^+$ analog resonance energies. No proton groups were observed corresponding to states with excitation energies greater than 3.3 MeV. The excitation functions measured for the inelastic proton groups are shown in Fig. 2. Angular distribution for the various groups on and off resonances are shown in Figs. 3–5.

The identification of the 2.31-MeV level in Sn^{116} is doubtful since it corresponds to a small peak partially obscured by a peak due to an impurity. However, it does seem to resonate at the $\frac{3}{2}^+$ resonance and was therefore considered to be a state of Sn^{116}. The level in Sn^{116} at 2.87 MeV, which is not seen at the $\frac{1}{2}^+$ resonance and only weakly at the $\frac{3}{2}^+$ resonance, might be the 2.845 level seen by Allan *et al.*[9] in the $Sn^{116}(p,p')$ reaction at 11 MeV.

In Sn^{122}, the states at 2.66 and 2.74 MeV have not been observed previously, either in the $Sn^{122}(p,p')$ reaction at 11 MeV by Allan[9] or in the $Sn^{122}(d,d')$ reaction at 15 MeV by Kim and Cohen.[10] The state at 2.86 MeV may correspond to the very weak state at 2.87 MeV seen in the (p,p') reaction at 11 MeV.[9]

In Sn^{124}, three very strong peaks were seen in addition to the strong 2^+ state at 1.13 MeV. All the peaks observed here, both the weak and strong peaks, were also identified at 11 MeV.[9] The peak at 2.69 MeV may correspond to two levels at 2.678 and 2.708 MeV seen in the (p,p') work at 11 MeV.[9]

In Sn^{116}, the 0^+ states identified by means of the (d,p) reaction[2] at 1.76 and 2.03 MeV, resonate more strongly at the $\frac{1}{2}^+$ resonance than at the $\frac{3}{2}^+$ resonance. Allan, Jones, Taylor, and Weinberg[7] observed similar behavior for the 0^+ states at 1.87 and 2.63 MeV in Sn^{120}. Such behavior is to be expected because of the lower-barrier-penetration probability of d waves as compared to s waves: In order to reach a 0^+ state from the $\frac{1}{2}^+$ analog state, a $l=0$ proton must be emitted while from the $\frac{3}{2}^+$ analog state, a $l=2$ proton must be emitted. The states at 2.08 and 2.66 MeV in Sn^{122} resonate at the $\frac{1}{2}^+$ isobaric analog resonance and not at the $\frac{3}{2}^+$ isobaric analog resonance. Likewise the level at 2.69 MeV in Sn^{124} resonates more strongly at the $\frac{1}{2}^+$ isobaric analog energy than at the $\frac{3}{2}^+$ energy. This behavior suggests that the 2.08- and 2.66-MeV states in Sn^{122} and the 2.69-MeV state in Sn^{124} may also have spin and parity 0^+. It should be noted, however, that the peak observed at 2.60 MeV in Sn^{116} does not show the same behavior, although a 0^+ level is known at 2.63 MeV from the (d,p) analysis.[2] This peak may correspond to two unresolved levels which resonate differently.

In the investigation of Allan, Jones, Morrison, Taylor, and Weinberg,[6] it appears that the collective 3^- states in Sn^{118} and Sn^{120} strongly resonate in the $Sn^{118}(p,p')$ and $Sn^{120}(p,p')$ reactions at the $\frac{3}{2}^+$ isobaric analog resonance. In the present experiment only a very small peak is identified as the 3^- level at the $\frac{3}{2}^+$ resonance in Sn^{122} and Sn^{124}. The spectrum of Sn^{116} does show a strong peak near the location of the 3^- state; however, the $Sn^{115}(d,p)$ reaction (Ref. 2) assigns a positive-parity, 1^+, 2^+, or 3^+ level very near this energy which could be mistaken for the 3^- state. In order to investigate this further, the spectra were measured at 130° for higher incident energies, $E_p=10$ MeV, where the 3^- state is known to be strongly excited. All spectra were measured at the lower resonance energies and at the higher energies in rapid succession in order to minimize the possibility of an error in energy calibration for the spectra. Figure 6 shows the spectrum for $Sn^{124}(p,p')$ measured at $E_p=10$ MeV. The 3^- state is correctly identified at the $\frac{3}{2}^+$ isobaric analog resonance as a very small peak. Perhaps the peaks observed in Sn^{116} and by Allan *et al.*[6,7] in Sn^{118} and Sn^{120} are not the 3^- states, but are the same positive-parity states which are observed in the (d,p) reactions.

The sums of the inelastic partial widths $\sum_{lj}\Gamma_{p'lj}$ are determined at the maximum of the resonance $(E=E_r)$,

[9] D. L. Allan, B. H. Armitage, and B. A. Doran, Nucl. Phys. **66**, 481 (1965).

[10] Y. S. Kim and B. L. Cohen, Phys. Rev. **142**, 788 (1966).

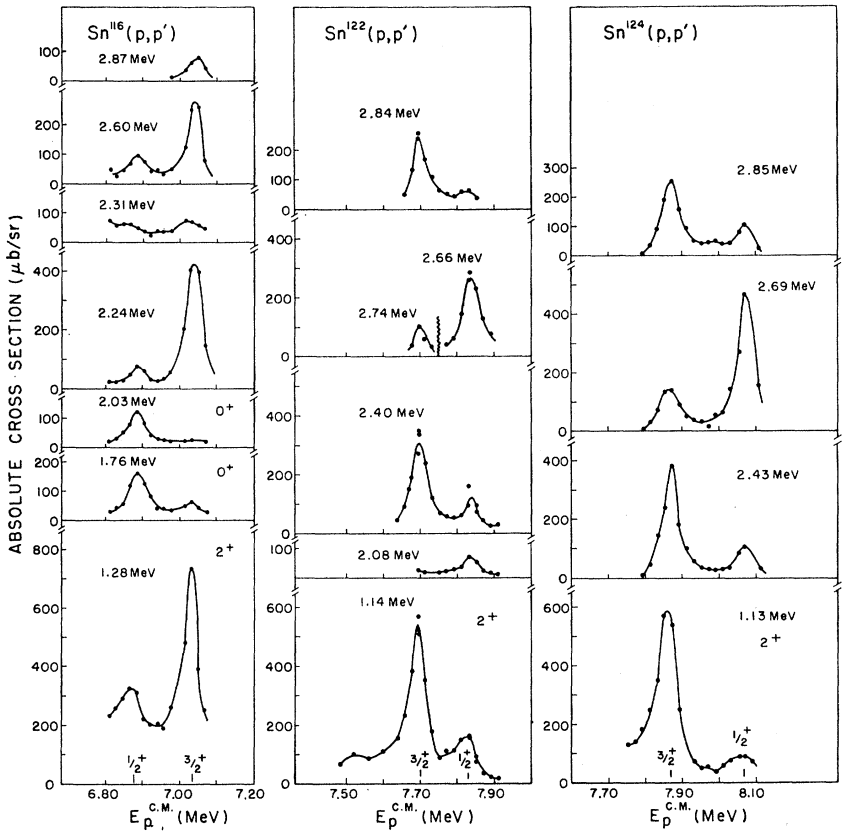

FIG. 2. The excitation functions measured for the inelastic proton groups. The 2.66- and 2.84-MeV states in Sn^{122} and the states of $Sn^{124}(p,p')$ were measured at $\theta=165°$; the remaining states shown were measured at $\theta=135°$.

using a single-level Breit-Wigner formula

$$\sum_{lj}\Gamma_{p'\,lj}=\frac{2\Gamma^2}{\lambda^2(2\mathcal{J}+1)\Gamma_p}\frac{\sigma_{pp'}}{4\pi}, \qquad (1)$$

where $\sigma_{pp'}$ is the total resonance cross section integrated over the angles, Γ_p is the partial width for the elastic proton, Γ is the total resonance width, and $\mathcal{J}$ is the spin of the isobaric analog state. The values for Γ and Γ_p used in expression (1) are those obtained from the elastic proton scattering analysis for the same analog states by Richard, Moore, Becker, and Fox[4] at Florida State University and are listed in Table IV.

In order to determine the total resonance cross sections $\sigma_{pp'}$, angular distributions were measured for the observed levels at the isobaric analog resonance energies and at off-resonance energies (Figs. 3–5). The angular distributions measured at off-resonance energies were used to determine nonresonant contributions to the cross sections. The nonresonant cross sections were then subtracted from the cross sections measured at the resonance energies in order to obtain the resultant resonance cross sections. This procedure appears to be valid for all states except the first excited 2^+ states, since the nonresonant cross sections for states other than the 2^+ states appears to be very small. However, the 2^+ states at the $\frac{1}{2}^+$ resonance clearly show interference effects with the nonresonant contributions to the cross sections for angles less than 90°. The extraction of $\sigma_{pp'}$ for the 2^+ states used only the data obtained for angles greater than 90°. The nonresonant cross sections for exciting the 2^+ states by the semiclassical Coulomb excitation process were calculated, using the following values for $B(E2)$: Sn^{116}, $B(E2)=(0.186\pm0.020)e^2\times10^{-48}$ cm^4 [11]; Sn^{122}, $B(E2)=(0.170\pm0.030)e^2\times10^{-48}$ cm^4 [12];

TABLE IV. The results obtained by Richard *et al.* (Ref. 4) from the elastic-proton-scattering analysis, which were used in the Breit-Wigner analysis of the inelastic-proton-scattering data.

E_p c.m. (MeV)	J^π	Γ_p (keV)	Γ (keV)
	$Sn^{116}(p,p)Sn^{116}$		
6.869	$\frac{1}{2}^+$	16.5	42
7.022	$\frac{3}{2}^+$	8.3	37
	$Sn^{122}(p,p)Sn^{122}$		
7.684	$\frac{3}{2}^+$	7	42
7.820	$\frac{1}{2}^+$	17	59
	$Sn^{124}(p,p)Sn^{124}$		
7.840	$\frac{3}{2}^+$	9	57
8.044	$\frac{1}{2}^+$	14	45

[11] Kleinfeld, de Boer, Covello-Moro, Bull. Am. Phys. Soc. 12, 564 (1967).

[12] D. G. Alkhazov, D. S. Andreev, K. I. Erokhina, and I. Kh. Lemberg, Zh. Eksperim. i Teor. Fiz. 33, 1347 (1950) [English transl.: Soviet Phys.—JETP 6, 1036 (1958)].

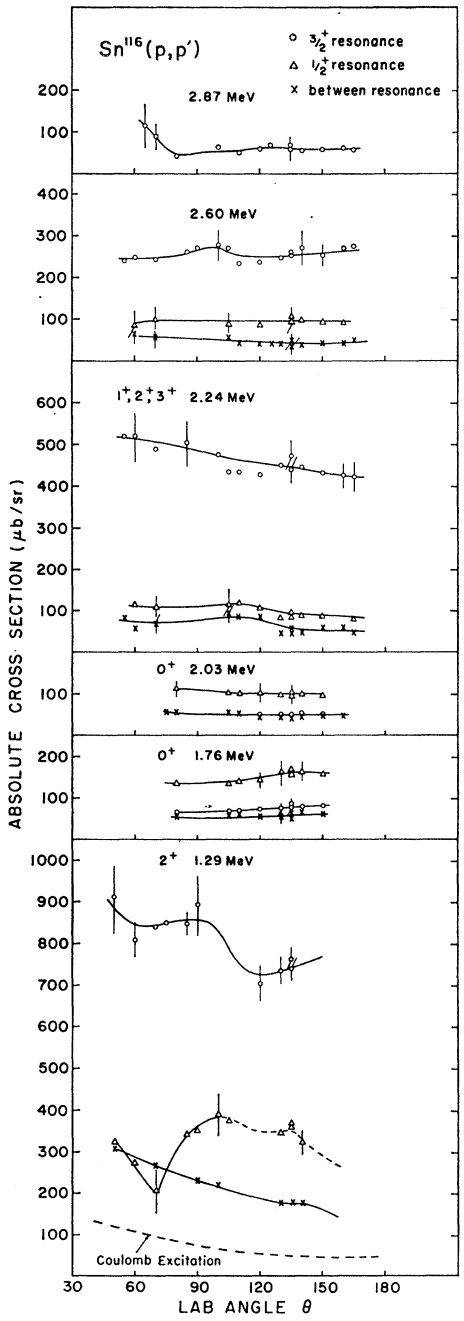

FIG. 3. The angular distributions for the strong inelastic peaks in Sn^{116}. Measurements were obtained on resonance energies and off resonance energies. The crosses × represent the values of the cross section between the $s_{1/2}$, $E_p^{c.m.}=6.87$ MeV, and $d_{3/2}$, $E_p^{c.m.}=7.02$ MeV, isobaric analog resonances. Shown also for the first 2^+ state is the expected Coulomb excitation cross section for a $B(E2)=(0.186\pm0.020)e^2\times10^{-48}$ cm^4 (Ref. 11).

Sn^{124}, $B(E2)=(0.165\pm0.0170)e^2\times10^{-48}$ cm^4 [11]; and are also shown in Figs. 3–5. In Sn^{122} and Sn^{124} the nonresonant cross section at 165° seems to be entirely due to the Coulomb excitation process. No data could be obtained for Sn^{116} at 165° because the C^{12} elastic peak was masking the 2^+ state. For more forward angles other processes such as direct nuclear interactions apparently contribute to the cross section.

Using the values of $\sigma_{pp'}$ and expression (1), only the sums of the inelastic partial widths can be determined.

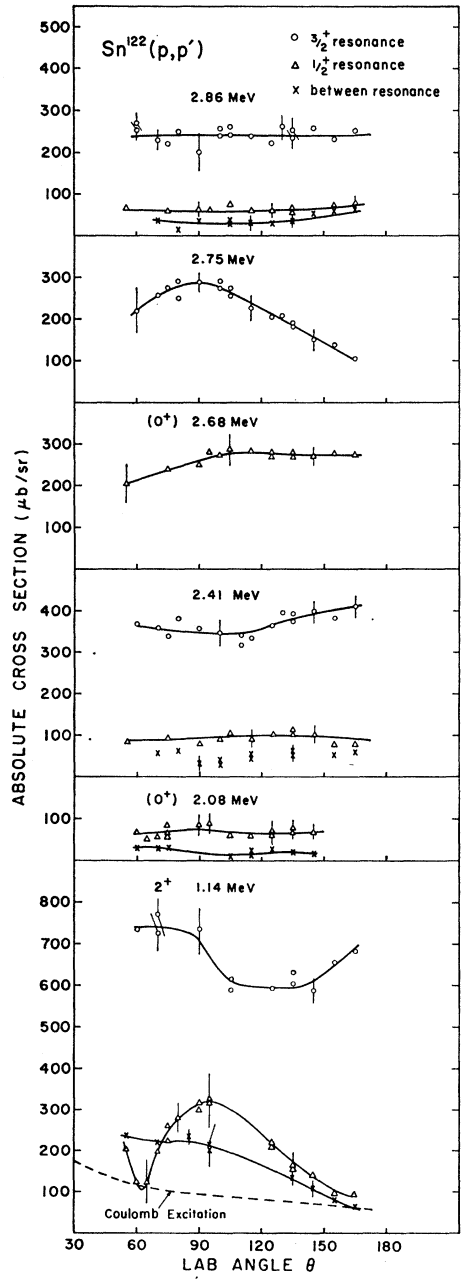

FIG. 4. The angular distributions for the strong inelastic peaks in Sn^{122}. Measurements were obtained on resonances energies and off resonance energies. The crosses × represent the values of the cross section between the $d_{3/2}$, $E_p^{c.m.}=7.68$ MeV and $s_{1/2}$, $E_p^{c.m.}=7.82$ MeV, isobaric analog resonances. Shown also for the first 2^+ state is the expected Coulomb excitation cross section for a $B(E2)=(0.170\pm0.030)e^2\times15^{-48}$ cm^4 (Ref. 12).

The results are listed in Tables I–III. The individual partial widths were in general not determined. For 0^+ final states only one value of orbital and total angular momenta l, j is allowed and the sum $\sum_{lj}\Gamma_{p'lj}$ reduces to one term. For the $\frac{1}{2}^+$ resonance usually only one value of l is allowed, e.g., in the decay to a 2^+ state $l=2$, $j=\frac{3}{2}$ or $\frac{5}{2}$, and the sum reduces to two terms. In general, one can try to obtain more information on the relative values of the $\Gamma_{p'lj}$ in the sum by analyzing the angular distributions. If one assumes that the reaction proceeds only via compound nucleus formation, the expressions of Blatt and Biedenharn[13] can be employed. However, this was not done for several reasons: (a) the neglect of direct reactions is not justified, especially for the first excited state (2^+); (b) The experimental errors in the angular distributions are not small, and no measurements were made for $\theta<50°$; (c) the experimental angular distributions show little structure, and are often almost isotropic; theoretically, all angular distributions on the $\frac{1}{2}^+$ resonance should be isotropic. It was felt that the sum of the partial widths extracted from the total cross section as described above was more reliable and, as will be seen below, would still allow comparison with theory.

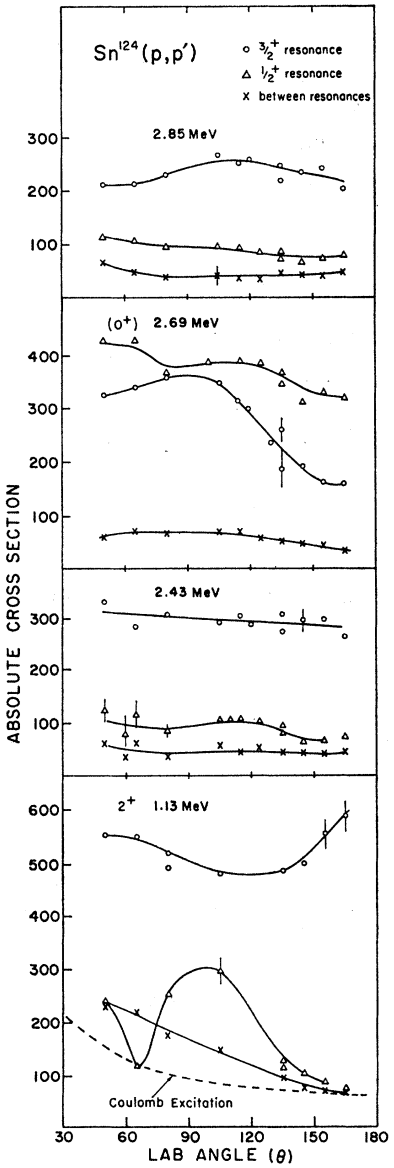

FIG. 5. The angular distributions for the strong inelastic peaks in Sn^{124}. Measurements were obtained on resonance energies and off resonance energies. The crosses × represent the value of the cross section between the $d_{3/2}$, $E_p^{c.m.}=7.84$ MeV and $s_{1/2}$, $E_p^{c.m.}=8.04$ MeV, isobaric analog resonances. Shown also for the first 2^+ is the expected Coulomb excitation cross section for a $B(E2)=(0.165\pm0.0170)e^2\times10^{-48}$ cm^4 (Ref. 11).

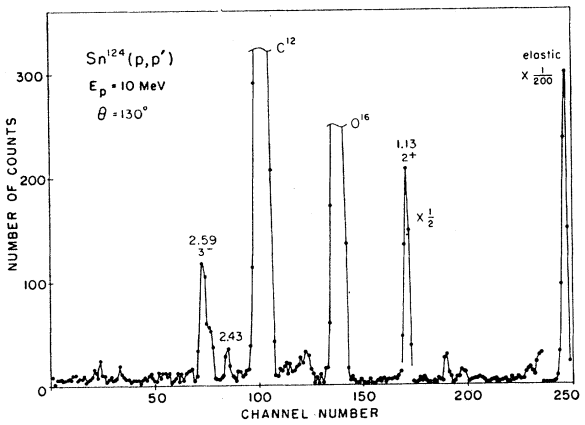

FIG. 6. The proton spectrum for Sn^{124} measured at $E_p=10$ MeV. The 3^- state can be seen to be strongly excited.

IV. DETERMINATION OF THE SINGLE-PARTICLE PARTIAL WIDTH

A very important quantity to be measured in nuclear-structure studies is the spectroscopic factor $S(l,j)$. A method similar to that suggested by Schiffer[14] and Andersen *et al.*[15] for extracting the spectroscopic factor from the partial width for an isobaric analog resonance is given by

$$S(l,j)=(2T_0+1)\Gamma_{plj}/\Gamma_{plj}^{sp}, \qquad (2)$$

where Γ_{plj}^{sp} is the calculated single-particle partial width, and Γ_{plj} is the measured partial width. The factor $2T_0+1$ is included to facilitate comparison with the spectroscopic factors for removal of a neutron from the parent state.

In order to determine Γ_{plj}^{sp}, a computer experiment is performed. Protons are scattered by a real potential of the form

$$V=V_{opt}+V_{Coul}, \qquad (3)$$

where V_{opt} is only the real part of an optical-model

[13] J. M. Blatt and L. C. Biedenharn, Rev. Mod. Phys. 24, 258 (1952).
[14] J. P. Schiffer, Nucl. Phys. 46, 246 (1963).
[15] B. L. Andersen, J. B. Bondorf, and B. S. Madsen, Phys. Letters 22, 651 (1966).

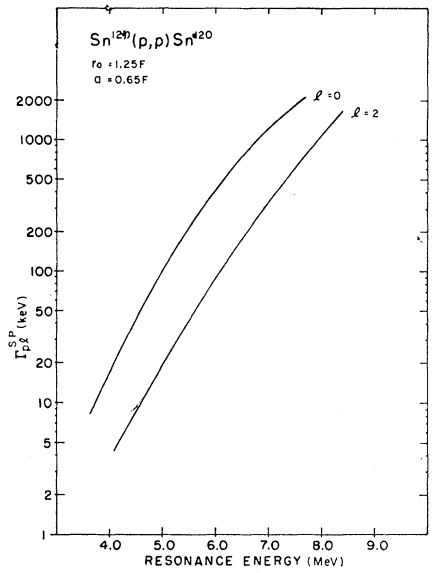

FIG. 7. The plot of the single-particle proton partial width Γ_{pl}^{sp} versus the resonance energy for $l=0$ and $l=2$.

potential of Saxon-Woods shape, and V_{Coul} is the Coulomb potential of a uniformly charged sphere.

The scattering goes through a resonance when the phase shift ϕ_{lj} in the l, j partial wave goes through 90°. Near resonance the cotangent of the phase varies linearly with the energy and the resonance width is defined by

$$\cot\phi_{lj}=\frac{2}{\Gamma_{plj}^{sp}}(E_r-E); \qquad (4)$$

E_r is the resonance energy, and E is the incident proton energy. Equation (4) defines the single-particle width to be used in calculating the spectroscopic factor, Eq. (2), when E_r in the computer experiment is the same as the experimentally measured resonance energy of the isobaric analog resonance. In order to make the computed and measured resonance energies coincide, the depth of the Saxon-Woods well was varied. Γ_{plj}^{sp} was obtained from the slope of the curve of $\cot\phi_{lj}$ versus E. The calculations were made using the distorted-wave Born approximation (DWBA) code JULIE[16] for several well depths (and therefore several resonance energies). The well depths ranged from 70 to 78 MeV; the radius parameters were held fixed at $r_0=r_c=1.25$ F; the diffuseness parameter was $a=0.65$ F. Plots of Γ_{pl}^{sp} versus E_r are shown in Fig. 7; there is no j dependence because no spin-orbit potential was included.

In earlier work,[17,18] a different method of estimating Γ_{plj}^{sp} was used (denoted as method I in Refs. 17 and 18): The radial wave function of the captured (but unbound) proton was approximated as being equal to the radial wave function of the bound neutron in the analog parent state. The present method (denoted as method II in Refs. 17 and 18) should be more accurate because it takes into account the unbound nature of the proton wave function and the effect of the nuclear potential on the barrier penetrabilities (in method I only Coulomb penetrabilities were considered).

TABLE V. A comparison of the relative spectroscopic factors from the $Sn^{116}(p,p')$ ($\frac{1}{2}^+$ isobaric analog resonance) and the $Sn^{117}(d,t)$ (Ref. 2) reactions. The values of J^π are those found in Ref. 2.

(d,t) E^* (MeV)	(p,p') E^* (MeV)	J^π	(d,t) $S_l(\frac{1}{2},J)_{rel}$	(p,p') $S_l(\frac{1}{2},J)_{rel}$
		$l=0$		
0.0	0.0	0^+	1	1
1.76	1.76	0^+	0.37	0.32
1.99	2.03	0^+	0.47	0.38
		$l=2$		
1.28	1.29	2^+	1	1
2.18	2.24	$(1^+,2^+,3^+)$	1.44	1.56

V. COMPARISON OF $Sn^{116}(p,p')$ AND $Sn^{117}(d,t)$ RESULTS

If the compound state observed in the (p,p') reaction is a perfect isobaric analog of a certain parent state, then the spectroscopic factors obtained from Eq. (2) should be equal to the spectroscopic factors for the (p,d) or (d,t) pickup reaction on a target which is in that parent state.[19] In the case of Sn^{116}, a comparison can be made between the $Sn^{116}(p,p')$ and $Sn^{117}(d,t)$ reactions, since Sn^{117} is available as a target. The ground state of Sn^{117} is $\frac{1}{2}^+$, so the $Sn^{117}(d,t)$ spectroscopic factors[2] are to be compared with the spectroscopic factors measured for the $Sn^{116}(p,p')$ reaction at the $\frac{1}{2}^+$ isobaric resonance.

A comparison of relative spectroscopic factors for the two reactions is made in Table V. The assignments of J^π listed in the table are those found in Ref. 2. The relative spectroscopic factors for the states formed by the transfer of an $l=0$ particle are normalized to the ground state, whereas the states formed by the transfer of an $l=2$ particle are normalized to the first 2^+ state. The agreement between the relative spectroscopic factors for the two reactions is seen to be quite good. Absolute values of S were not obtained in the (d,t) experiment.

VI. COMPARISON OF RESULTS WITH THEORETICAL PREDICTIONS

Spectroscopic factors for both the $\frac{1}{2}^+$ and $\frac{3}{2}^+$ isobaric analog resonances can be compared with the spectroscopic factors which can be predicted if the wave functions for the initial and final states are available.

[16] R. H. Bassel, R. M. Drisko, and G. R. Satchler, Oak Ridge National Laboratory Report No. ORNL-3240, 1962 (unpublished).
[17] E. W. Hamburger, B. L. Cohen, J. Kremenek, J. B. Moorhead, and C. Shin (to be published).
[18] E. Schneid, PhD thesis, University of Pittsburgh, 1966 (unpublished).
[19] D. Robson, Phys. Rev. 137, 535 (1965).

Using the wave functions of Kuo, Baranger, and Baranger,[3] E. Baranger[20] calculated the corresponding spectroscopic factors involved for the $\frac{1}{2}^+$ and $\frac{3}{2}^+$ isobaric analog resonances in Sb^{117}, Sb^{123}, and Sb^{125}.

If it is assumed that the parent state in the odd tin isotope is a pure one-quasiparticle state and that the state in the even nucleus is a pure two-quasiparticle state, then the work of Baranger and Kuo[21] gives the following expression for the spectroscopic factor for proton emission from the analog state to an excited state k of the even nucleus:

$$S_{lj}(J,\mathcal{J})=V_j^2\frac{2J+1}{2\mathcal{J}+1}\psi^{(k)}(\mathcal{J}jJ)(1+\delta\mathcal{J}j),$$

where V_j^2 is the fullness of the single-particle state j in the odd nucleus, J is the total angular momentum of the two-quasiparticle state (k) in the even nucleus, $\mathcal{J}$ is the total angular momentum of the analog state, $\psi^{(k)}(\mathcal{J}jJ)$ is the amplitude for finding, in the kth eigenfunction of the even nucleus, that state consisting of two quasiparticles in states $\mathcal{J}$ and j, and δ is the Kronecker delta function. The spectroscopic factors were calculated for $s_{1/2}$, $d_{3/2}$, $d_{5/2}$, and $g_{7/2}$ quasiparticles and for final states with $J^\pi=0^+$, 1^+, 2^+, 3^+, and 4^+.

Since only the sum of the partial widths was obtained from the data, experimental spectroscopic factors were not determined. However, using the spectroscopic factors calculated by E. Baranger, the values of $\Gamma_{plj}{}^{sp}$ determined in Sec. IV, and relation (2), a sum of theoretical partial widths can be obtained and compared to the experimental results.

Tables VI–VIII give the theoretical predictions for the partial widths. These tables list the excitation energies for the theoretical states of the residual nucleus

TABLE VI. The theoretical predictions for the $Sn^{116}(p,p')$ reactions at the $\frac{1}{2}^+$ and $\frac{3}{2}^+$ isobaric analog resonances. This table lists the excitation energies for the theoretical two-quasiparticle states of the residual nucleus, the J^π for these states, the values of l and j for the transferred particles, the spectroscopic factors calculated by Baranger (Ref. 20), and the partial widths calculated using Eq. (2).

		$\frac{3}{2}^+$ analog state			$\frac{1}{2}^+$ analog state		
E^* (MeV)	J^π	l,j	$S(l,j)$	Γ_{plj} (keV)	l,j	$S(l,j)$	Γ_{plj} (keV)
0.0	0^+	$2,\frac{3}{2}$	0.815	16.8	$0,\frac{1}{2}$	0.533	33.0
1.471	0^+	$2,\frac{3}{2}$	0.015	0.04	$0,\frac{1}{2}$	0.144	1.48
1.534	2^+	$0,\frac{1}{2}$	0.116	1.29	$2,\frac{3}{2}$	0.106	0.40
		$2,\frac{3}{2}$	0.061	0.18	$2,\frac{5}{2}$	0.091	
		$2,\frac{5}{2}$	0.011				
		$4,\frac{7}{2}$	0.049	...			
2.081	0^+	$2,\frac{3}{2}$	0.007	0.001	$0,\frac{1}{2}$	0.028	0.11
2.362	0^+	$2,\frac{3}{2}$	0.069	0.05	$0,\frac{1}{2}$	0.236	0.51
2.404	2^+	$0,\frac{1}{2}$	0.152	0.45	$2,\frac{3}{2}$	0.139	0.07
		$2,\frac{3}{2}$	0.253	0.15	$2,\frac{5}{2}$	0.014	
		$2,\frac{5}{2}$	0.001	...			
		$4,\frac{7}{2}$	0.003	...			
2.468	4^+	$2,\frac{5}{2}$	0.012	0.004	$4,\frac{7}{2}$	0.033	...
		$4,\frac{7}{2}$	0.033	...			
2.678	1^+	$0,\frac{1}{2}$	0.410	1.06	$2,\frac{3}{2}$	0.376	0.10
		$2,\frac{5}{2}$	0.000	...			
2.978	2^+	$0,\frac{1}{2}$	0.062	0.066	$2,\frac{3}{2}$	0.056	0.03
		$2,\frac{3}{2}$	0.015	0.005	$2,\frac{5}{2}$	0.138	
		$2,\frac{5}{2}$	0.009				
		$4,\frac{7}{2}$	0.064	...			

[20] E. Baranger (private communication).

TABLE VII. The theoretical predictions for the $Sn^{122}(p,p')$ reaction at the $\frac{1}{2}^+$ and $\frac{3}{2}^+$ isobaric analog resonances. See also caption for Table VI.

		$\frac{3}{2}^+$ analog state			$\frac{1}{2}^+$ analog state		
E^* (MeV)	J^π	l,j	$S(l,j)$	Γ_{plj} (keV)	l,j	$S(l,j)$	Γ_{plj} (keV)
0.0	0^+	$2,\frac{3}{2}$	0.449	14.6	$0,\frac{1}{2}$	0.211	21.5
1.150	2^+	$0,\frac{1}{2}$	0.125	4.24	$2,\frac{3}{2}$	0.185	1.73
		$2,\frac{3}{2}$	0.209	1.75	$2,\frac{5}{2}$	0.058	0.54
		$2,\frac{5}{2}$	0.013				
		$4,\frac{7}{2}$	0.045	...			
1.567	0^+	$2,\frac{3}{2}$	0.123	0.55	$0,\frac{1}{2}$	0.200	4.87
2.247	4^+	$2,\frac{5}{2}$	0.016	0.027	$4,\frac{7}{2}$	0.014	...
		$4,\frac{7}{2}$	0.010	...			
2.466	2^+	$0,\frac{1}{2}$	0.005	0.025	$2,\frac{3}{2}$	0.007	0.013
		$2,\frac{3}{2}$	1.211	1.47	$2,\frac{5}{2}$	0.002	
		$2,\frac{5}{2}$	...	...			
		$4,\frac{7}{2}$	...	...			
2.640	0^+	$2,\frac{3}{2}$	0.103	0.096	$0,\frac{1}{2}$	0.540	2.82
2.742	2^+	$0,\frac{1}{2}$	0.851	3.11	$2,\frac{3}{2}$	1.26	1.23
		$2,\frac{3}{2}$	0.085	0.067	$2,\frac{5}{2}$	0.009	
		$2,\frac{5}{2}$	...	...			
		$4,\frac{7}{2}$	0.008	...			
2.837	1^+	$0,\frac{1}{2}$	0.617	1.93	$2,\frac{3}{2}$	0.912	0.76
		$2,\frac{5}{2}$	...	...			

TABLE VIII. The theoretical predictions for the $Sn^{124}(p,p')$ reaction at the $\frac{1}{2}^+$ and $\frac{3}{2}^+$ isobaric analog resonances. See also caption for Table VI.

		$\frac{3}{2}^+$ analog state			$\frac{1}{2}^+$ analog state		
E^* (MeV)	J^π	l,j	$S(l,j)$	Γ_{plj} (keV)	l,j	$S(l,j)$	Γ_{plj} (keV)
0.0	0^+	$2,\frac{3}{2}$	0.334	12.3	$0,\frac{1}{2}$	0.145	16.3
1.148	2^+	$0,\frac{1}{2}$	0.131	4.62	$2,\frac{3}{2}$	0.214	3.08
		$2,\frac{3}{2}$	0.265	1.91	$2,\frac{5}{2}$	0.048	
		$2,\frac{5}{2}$	0.012				
		$4,\frac{7}{2}$	0.041	...			
1.576	0^+	$2,\frac{3}{2}$	0.184	0.92	$0,\frac{1}{2}$	0.161	4.56
2.216	4^+	$2,\frac{5}{2}$	0.015	0.02	$4,\frac{7}{2}$	0.012	...
		$4,\frac{7}{2}$	0.008	...			
2.403	2^+	$0,\frac{1}{2}$	0.008	...	$2,\frac{3}{2}$	0.013	0.03
		$2,\frac{3}{2}$	1.40	2.20	$2,\frac{5}{2}$	0.003	
		$2,\frac{5}{2}$	0.001	...			
		$4,\frac{7}{2}$	...	...			
2.689	0^+	$2,\frac{3}{2}$	0.093	0.095	$0,\frac{1}{2}$	0.653	4.05
2.708	2^+	$0,\frac{1}{2}$	0.916	4.13	$2,\frac{3}{2}$	1.50	2.05
		$2,\frac{3}{2}$	0.114	0.11	$2,\frac{5}{2}$	0.009	
		$2,\frac{5}{2}$	0.001				
		$4,\frac{7}{2}$	0.008	...			
2.813	1^+	$0,\frac{1}{2}$	0.661	2.65	$2,\frac{3}{2}$	1.08	1.26
		$2,\frac{5}{2}$	...	...			

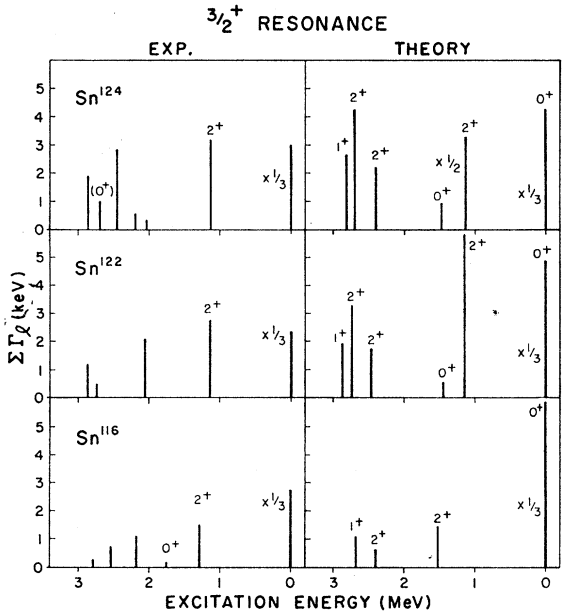

FIG. 8. A comparison between the experimental sums of partial widths measured at the $\frac{3}{2}^+$ isobaric analog resonances and the sums of theoretical partial widths predicted by shell-model calculations. The theoretical results are those listed in Tables VI–VIII.

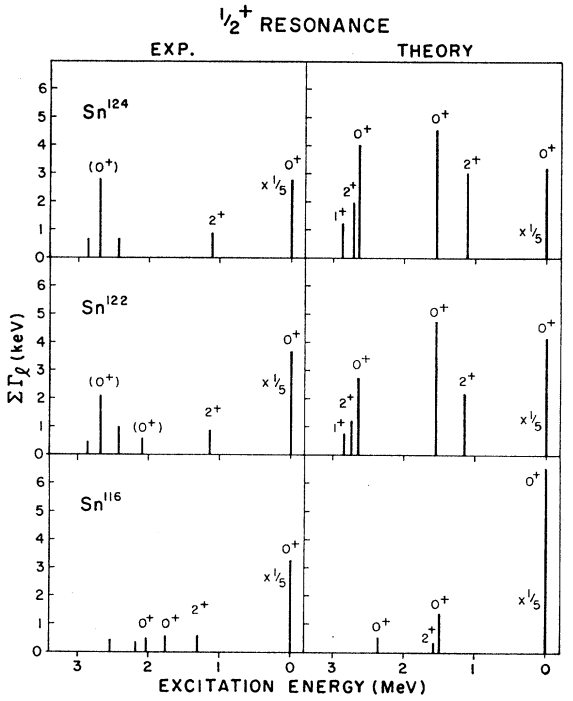

FIG. 9. A comparison between the experimental sums of partial widths measured at the $\frac{1}{2}^+$ isobaric analog resonances and the sums of theoretical partial widths predicted by shell-model calculations. The theoretical results are those listed in Tables VI–VIII.

below 3.3 MeV, the J^π for these states, the values of l and j for the transferred particles, the spectroscopic factors, and the partial widths.

The wave functions are those calculated with the parameters of Table 5a of Ref. 3. The sensitivity of the results to the choice of parameters was checked[20] by calculating the spectroscopic factors also with the parameters of Table 5e of Ref. 3. The larger spectroscopic factors in the two calculations, $S>0.1$, usually agree within 10%; in a few cases there are 25% discrepancies, and above 4-MeV excitation energy in the even nucleus, larger disagreements appear. However, no data were obtained above 4-MeV excitation.

The comparisons between the experimental results and the sums of the partial width listed in Tables VI–VIII are shown in Figs. 8 and 9. It should be noted that the spins and parities of all the experimental states are not yet known so that a level-by-level comparison cannot be made. The over-all agreement between experiment and theory is good; it is comparable to the agreement found by Baranger and Kuo[21] between the experimental stripping spectroscopic factors,[2] and the predictions of the wave functions of Baranger, Kuo, and Baranger. In particular, the large partial widths measured to excited states between 2- and 3-MeV excitation energy are correctly predicted by the theory. A conspicuous disagreement concerns the 0^+ states at ~1.5-MeV excitation in Sn^{122} and Sn^{124} which are predicted to be strongly excited at the $\frac{1}{2}^+$ resonance but are not observed experimentally. Otherwise, the agreement is as good as can be expected from the crudeness of the theory, and from the method of extracting the partial widths and of estimating the single-particle widths.

[21] E. Baranger and T. T. S. Kuo (to be published).

ACKNOWLEDGMENTS

The authors wish to thank C. Shin for his assistance in the accumulation and analysis of the data, and the technical staff for the operation of the Tandem Van de Graaff. The cooperation of Dr. E. Baranger, who furnished the theoretical spectroscopic factors, was invaluable and greatly appreciated.

The calculations reported in this article were performed at the University of Pittsburgh computation center which is partially supported by the National Science Foundation under Grant No. G-11309.